

# ON THE POSSIBILITY OF SIMPLE PARALLEL COMPUTING OF VORONOI DIAGRAMS AND DELAUNAY GRAPHS

DANIEL REEM

**ABSTRACT.** The Voronoi diagram is a widely used data structure. The theory of algorithms for computing Euclidean Voronoi diagrams of point sites is rich and useful, with several different and important algorithms. However, this theory has been quite steady during the last few decades in the sense that new algorithms have not entered the game. In addition, most of the known algorithms are sequential in nature and hence cast inherent difficulties on the possibility to compute the diagram in parallel. This paper presents a new and simple algorithm which enables the (combinatorial) computation of the diagram. The algorithm is significantly different from previous ones and some of the involved concepts in it are in the spirit of linear programming and optics. Parallel implementation is naturally supported since each Voronoi cell can be computed independently of the other cells. A new combinatorial structure for representing the cells (and any convex polytope) is described along the way and the computation of the induced Delaunay graph is obtained almost automatically.

---

*Date:* March 18, 2012.

*2010 Mathematics Subject Classification.* 68U05, 68W10, 65D18.

*Key words and phrases.* Algorithm, combinatorial representation, cone, conic beam, Delaunay graph, parallel computing, ray, subface, vertex, Voronoi diagram.

IMPA - Instituto Nacional de Matemática Pura e Aplicada, Estrada Dona Castorina 110, Jardim Botânico, CEP 22460-320, Rio de Janeiro, RJ, Brazil.

E-mail: dream@impa.br .

## 1. INTRODUCTION

1.1. **Background.** In its simplest and widespread form, the Voronoi diagram (the Voronoi tessellation, Dirichlet tessellations) is a certain decomposition of the Euclidean plane (or a region  $X$  in the plane) into cells induced by a collection of distinct points  $p_1, \dots, p_n$  (called the sites or the generators) and the Euclidean distance. More precisely, the Voronoi cell  $R_k$  associated with the site  $p_k$  is the set of all the points in  $X$  whose distance to  $p_k$  is not greater than their distance to the other sites  $p_j$ ,  $j \neq k$ . This definition can be easily generalized to other setting, e.g.,  $\mathbb{R}^m$ , sites having more general form, various distance functions, etc.

Because they appear in many fields in science and technology and have numerous applications, these diagrams have attracted a lot of attention during the last 4 decades and even before [6, 7, 41, 29], especially in the case of 2-dimensional Euclidean Voronoi diagrams of point sites. In particular, many algorithms for computing these diagrams in the above mentioned setting have been published. Among them we mention the naive method [41, pp. 230-233], the divide-and-conquer method [3], [41, pp. 251-257], [49], the incremental method [31], [32], [40], [41, pp. 242-251], the plane sweep method [27], [41, pp. 257-264], methods based on geometric transforms such as convex hulls [8, 12, 13, 14, 25] or Delaunay tessellations [33], [41, pp. 275-80], methods based on lower envelopes [48], [50, p. 241] and methods for very specific configurations [2].

It can be seen that the theory of algorithms for computing 2D Euclidean Voronoi diagrams of point sites is rich and useful, with many different and important algorithms and analyses. However, this theory has been quite steady during the last decades. Some valuable improvements and variations in known algorithms have appeared, but new algorithms have not entered the game.

Another property of this theory is that most of the known algorithms are sequential in nature and they cannot compute each of the cells independently of the other ones. Instead, they consider the diagram as a combinatorial structure and compute it as a whole in a sequential way. This fact casts inherent difficulties on any attempt to implement these algorithms in a parallel computing environment. It is therefore not surprising to see claims such as “Parallelizing algorithms in computational geometry usually is a complicated task since many of the techniques used (incremental insertion or plane sweep, for instance) seem inherently sequential” [6, p. 367] or “It is seldom obvious how to generate parallel algorithms in this area [computational geometry] since popular techniques such as contour tracing, plane sweeping, or gift wrapping involve an explicitly sequential (iterative) approach” [1, p. 293].

As a result of what written above, there is something noteworthy in the fact that a corresponding theory for parallelizing the computation of Voronoi diagrams has been developed [1, 16, 17, 26, 30, 35, 38, 43] (see also [6, pp. 367-369]) and has even been extended to related geometric structures such as the Delaunay triangulation [4, 5, 11, 19, 28, 39, 45, 47, 54, 55, 56]. In the works mentioned above the idea is to somehow share the work between the many processing units (under certain assumptions on the computational model), but because of the sequential nature of

the involved algorithms, these processing units must cooperate between themselves and cannot work independently. Unfortunately, the above mentioned sequential nature of the involved algorithms complicates the implementation of many of these parallelizing attempts. In addition, a common assumption in the above works is that there are many processing units, e.g.,  $O(n)$ , where  $n$  is the number of sites. This obviously casts difficulties on a practical implementation when the number of sites is large. The case of geometric structures related to Voronoi diagrams is similar: they are either based on the former works or vice versa, or they use somewhat similar techniques or similar assumptions on the computational models and the number of processing units.

The motivation for developing parallel-in-nature algorithms for computational tasks stems from several natural reasons. One important reason is the ability to compute in a fast manner much larger inputs than computed today, in numerous fields, or to perform in a fast way computations which require many iterations, such as centroidal Voronoi diagrams (CVD) [23, 24]. Another reason is that in recent years most of the computing devices (various types of computers, cell phones, graphic processors, etc.) arrive with several (sometimes with hundreds or even thousands) processing units (cores) which are just waiting for being used. Large networks of such computing devices can be also used for parallel computing tasks.

Taking into account all of the above, it is natural to ask whether there exists an algorithm which can compute each of the Voronoi cells independently of the other ones, and hence can provide a simple way to compute the Voronoi diagram in parallel. To the best of our knowledge, only one such an algorithm has been discussed in the literature, namely the naive one which computes each of the cells by intersecting corresponding halfspaces [41, pp. 230-233]. This (very) veteran algorithm is simple, but it is relatively slow:  $O(n^2 \log(n))$  for the whole diagram of  $n$  sites in the worst case (assuming 1 processing unit is involved). As claimed in [10], on the average (under the assumption of uniform distribution) its time complexity should behave as  $O(n)$ . We have not seen any implementation which confirms this, and, as a matter of fact, it seems that in general this algorithm is not used frequently. However, a variation of this naive algorithm for the Delaunay triangulation case has appeared very recently in [15], but a careful verification of the data given there shows that when the sites are generated according to the uniform distribution, the implementation behaves in a way which is worse than  $O(n)$ .

Recently [44], a new algorithm which allows the approximate computation of Voronoi diagrams in a general setting (general sites, general norms, general dimension) was introduced. This algorithm is based on the possibility to represent each cell as a union of rays (line segments), and it approximates the cells by considering a plurality of approximating rays. See Figures 1-2 for an illustration. This algorithm allows the computation of each cell independently of the other ones. However, although in principle the algorithm may compute the combinatorial structure of the cell (e.g., its vertices), this is done in a non-immediate and non-efficient way, since for doing this it needs to somehow detect the corresponding combinatorial components

and for achieving this task many rays should be considered and the information obtained from them should be analyzed correctly. What is not clear in advance is to which direction to shoot a ray such that it will hit a vertex exactly. It is therefore natural to ask whether this algorithm can somehow be modified in a such a way that it will allow a simple and efficient computation of the combinatorial structure.

**1.2. Contribution of this work.** This paper presents and analyzes a new algorithm which enables the combinatorial computation of 2D Euclidean Voronoi diagrams of point sites, where each cell is computed independently of the other ones. In fact, even portions of the same cell can be computed independently of other portions. Parallel implementation is therefore naturally supported. The algorithm is significantly different from previous ones and some of the involved concepts are in the spirit of linear programming and optics. In contrast to many algorithms, the sites can form any configuration (no “general position” assumption to avoid degenerate cases is made). A new combinatorial structure for representing the cells (and any convex polytope) is described along the way, and the computation of the corresponding Delaunay graph (Delaunay triangulation) is obtained almost automatically. The time complexity of the algorithm, as a serial one (one processing unit) for the whole diagram, is bounded above by  $O(n^2)$ . This upper bound on the time complexity is better than the one of the naive algorithm and it is not known to be tight. The actual behavior is in fact more or less linear when the sites are distributed uniformly. It should be emphasized that this paper is theoretical. Issues related to implementation and experimental results will be discussed elsewhere.

**1.3. The structure of the paper.** In Section 2 the notation, terminology and several tools are introduced. In Section 3 a schematic description of the algorithm is given. A detailed description of the algorithm is given in Section 4. A method for finding endpoints in an exact way is described in Section 5. The method of storing the data as well as a discussion on some combinatorial issues are described in Section 6. In Section 7 it is mentioned briefly how the Delaunay graph can be extracted almost automatically from the stored data. The possibility to extend the results to higher dimensions, as well as a new combinatorial representation for the cells (in any dimension), are discussed in Section 8. A discussion on several issues, e.g., on the time complexity, is given in Section 9. Proofs of some claims are given in Section 10.

## 2. PRELIMINARIES

In this section we present the notation and basic definitions used later, as well as some helpful tools. Our world  $X$  is a convex and compact polygon in the Euclidean plane  $(\mathbb{R}^2, |\cdot|)$ . The induced metric is  $d(x, y) = |x - y|$ . We denote by  $[p, x]$  and  $[p, x)$  the closed and half open line segments connecting  $p$  and  $x$ , i.e., the sets  $\{p + t(x - p) : t \in [0, 1]\}$  and  $\{p + t(x - p) : t \in [0, 1)\}$  respectively. The inner product between the vectors  $x = (x_1, x_2)$  and  $y = (y_1, y_2)$  is  $\langle x, y \rangle = \sum_{i=1}^2 x_i y_i$ . A nonnegative linear cone emanating from a point  $p$  and generated by the vectors

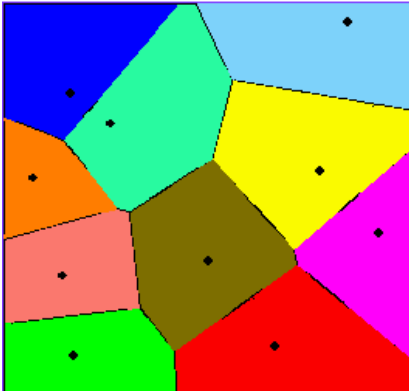


FIGURE 1. A Voronoi diagram of 10 point sites in a square in the Euclidean plane.

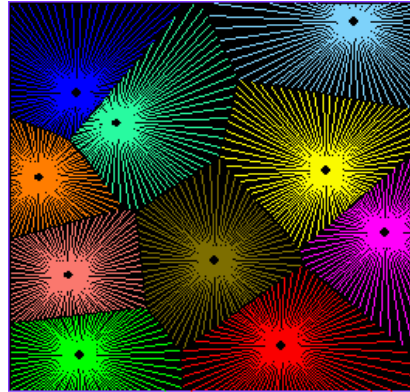


FIGURE 2. Each of the cells of Figure 1 is approximated using 80 rays.

$t_1, t_2$  is the set  $\{p + \sum_{i=1}^2 \lambda_i t_i : \lambda_i \geq 0, i = 1, 2\}$ . Lines are denoted by  $L, M$ , etc. A facet of a polygon located on a corresponding line  $L$  is denoted by  $\tilde{L}$ . In dimension 2 a face of the cell is just an edge and we alternatively use the names “edge”, “side”, “face”, or “facet” for describing this notion. The sites are denoted by  $p_k, k \in K = \{1, \dots, n\}$ . They are assumed to be points and  $p_k \neq p_j$  whenever  $k \neq j$ .

**Definition 2.1.** *The Voronoi diagram of the tuple of point sites  $(p_k)_{k=1}^n$  contained in the region  $X$  is the tuple  $(R_k)_{k=1}^n$  of subsets  $R_k \subseteq X$  where, for each  $k \in K = \{1, \dots, n\}$ ,*

$$R_k = \{x \in X : d(x, p_k) \leq d(x, p_j) \quad \forall j \in K, j \neq k\}.$$

*In other words, the Voronoi cell  $R_k$  associated with the site  $p_k$  is the set of all  $x \in X$  whose distance to  $p_k$  is not greater than their distance to the other sites  $p_j$ .*

The definition of the Voronoi diagram is analytic. However, it can be easily seen that each cell  $R_k$  is the intersection of the world  $X$  with halfplanes: the halfplanes  $\{x \in \mathbb{R}^2 : d(x, p_k) \leq d(x, p_j), j \neq k\}$ . Thus each cell is a closed and convex set which can be represented using its combinatorial structure, namely its vertices and sides. Because of this property the traditional approach to Voronoi diagrams is combinatorial.

In a recent work [44], a different representation of the cells was introduced, suggesting to consider each of the cells as a union of rays (lines segments). This representation is related to, but different from, the fact that the Voronoi cells are star-shaped. The theory of Voronoi diagrams in general and of algorithms for computing Voronoi diagrams in particular, is very diverse, with plenty of interesting and important facts and ideas. In particular, the star-shaped property of the cells is a well-known fact. However (the following sentences were added as a result of a certain criticism the author has received), to the best of our knowledge, and this is said after an extensive search that we have made in the literature (for many years)

and after conversations with (or in front of) many experts (in various scientific and technological domains), there has been no attempt or any kind of mention (even informal ones) before [44] of the possibility to represent the Voronoi cells in the way described in Theorem 2.2 and to use any kind of ray-shooting techniques to compute (possibly approximately) these cells. Phenomena (even basic ones) which have the potential to be valuable can be discovered despite a certain amount of research because there does not exist any known algorithm which enables the discovery of all of such phenomena (or at least decides without any doubt that all of such phenomena have been discovered) assuming certain parameters such as time and work are known in advance. New discoveries and new insights regarding known facts are being made by scientists all the time. This is an essential part of Science as a whole. The discovery of an algorithm of the type mentioned above (or at least its theoretical existence), will be, in a sense, something much better than a polynomial time algorithm for solving NP-complete problems.

**Theorem 2.2.** *The Voronoi cell  $R_k$  of a site  $p = p_k$  is a union of rays emanating from  $p$  in various directions. More precisely, denote  $A = \bigcup_{j \neq k} \{p_j\}$ . Given a unit vector  $\theta$ , let*

$$T(\theta, p) = \sup\{t \in [0, \infty) : p + t\theta \in X \text{ and } d(p + t\theta, p) \leq d(p + t\theta, A)\}. \quad (2.1)$$

*The point  $p + T(\theta, p)\theta$  is the endpoint corresponding to the ray emanating from  $p$  in the direction of  $\theta$ . Then*

$$R_k = \bigcup_{|\theta|=1} [p, p + T(\theta, p)\theta].$$

This representation actually holds (after simple modifications) in a more general setting (any norm, any dimension, sites of a general form, etc.) and it shows that by “shooting” enough rays one can obtain a fairly good approximation of the cells (see Figures 1-2). However, as explained in Section 1, it is not immediate to obtain the combinatorial structure from this representation. Nevertheless, it will be shown later how the idea of shooting rays can indeed be used for obtaining this structure.

### 3. A SCHEMATIC DESCRIPTION OF THE ALGORITHM

In this section we present a schematic description of the algorithm for computing the Voronoi cells. The method is based on the fact that the cell of some point site  $p = p_k$  is a convex polygon whose boundary consists of vertices and edges. A detailed description, including a pseudo code and illustrations, are given in Section 4. Some of the involved concepts are in the spirit of optics and linear programming.

A high-level description of the method is given below. Recall again that for a unit vector  $\theta$ , the point  $p + T(\theta, p)\theta$  is the endpoint corresponding to the ray emanating from  $p$  in the direction of  $\theta$  (see Figure 2).

**Method 3.1.** *A high level description:*

- **Input:** A site  $p$ ;
  - **Output:** The (combinatorial) Voronoi cell of  $p$ ;
- (1) Think of  $p$  as a light source;
  - (2) emanate a (linear) conic beam of light from  $p$  using a simplex;
  - (3) detect iteratively (by possibly dividing the cone to suncones) all possible vertices (and additional related combinatorial information) inside this beam using corresponding endpoints and an associated system of equations;
  - (4) continue the process with other beams until the whole space around  $p$  is covered;

The actual generation and handling of the (sub)cones is done using a simplex (triangle) located around  $p$ . The boundary of this simplex is initially composed of one-dimensional faces, and later these faces are composed of subfaces, when we narrow the search to subcones (sub-beams). Each such a subface induces a cone: the cone generated by the rays which pass via the corners of the subface; See Figure 5. Each such a corner induces a unit vector (denoted by  $\theta$ ) which points in its direction (from  $p$ ). Once the corresponding unit vector is known, then so is the ray in its direction.

The system of equations mentioned above (Step (3)) is

$$B\lambda = H, \tag{3.1}$$

where the vector of unknowns is  $\lambda = (\lambda_1, \lambda_2)$ ,  $B$  is the 2 by 2 matrix with entries  $B_{ij} = \langle N_i, T_j \rangle$  and  $H$  is a 2-dimensional vector with entries  $H_i = \langle N_i, T_i \rangle, i, j \in \{1, 2\}$ . The notation  $T_i = T(\theta_i, p)\theta_i$  means the vector in direction  $\theta$  whose length is the distance from  $p$  to the endpoint  $p + T_i$ . The 2-dimensional vector  $N_i$  is a normal to the line  $L_i = \{x : \langle N_i, x \rangle = c_i = \langle N_i, p + T_i \rangle\}$  on which the endpoint  $p + T_i$  is located.

Equation (3.1) has a simple geometric meaning: the point  $u = p + \sum_{i=1}^2 \lambda_i T_i$  is in the intersection of the lines  $L_1, L_2$  if and only if  $\lambda$  solves (3.1). If we want to restrict ourselves to the cone generated by the corresponding rays, then we consider only the nonnegative solutions of (3.1), i.e.,  $\lambda_i \geq 0$  for all  $i = 1, 2$ . If equation (3.1) has a unique nonnegative solution  $\lambda$ , then this means that  $u$  is a point in the cone which is a candidate to be a vertex of the cell, since it may be (but is not necessary) in the intersection of the corresponding 2 different facets located on the lines  $L_i$ . If, in addition,  $u$  is known to be in the cell, then it is indeed a vertex.

#### 4. A DETAILED DESCRIPTION OF THE ALGORITHM

Method 3.1 is described in a detailed way in this section, starting from the next paragraph. See page 9 for a pseudo-code and Figures 3-4 for an illustration. An additional related illustration is given in Figure 8.

First, we create the 3 unit vectors  $\theta_i$  corresponding to a simplex around the point  $p$ . After choosing a simplex subface, shooting the two rays in the direction of  $\theta_i, i = 1, 2$ , finding the endpoints  $p + T_i$  (using, e.g., Method 5.1 in Section 5; here

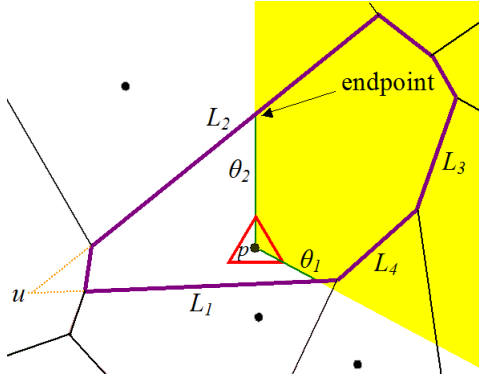


FIGURE 3. Illustration of the algorithm. The cone generated by the subspace  $\{\theta_1, \theta_2\}$  is shown. The intersection between  $L_1$  and  $L_2$  is a point outside the cone and hence the cone is divided. The next two subspaces are  $\{\theta_1, \theta_3\}$ ,  $\{\theta_2, \theta_3\}$ .

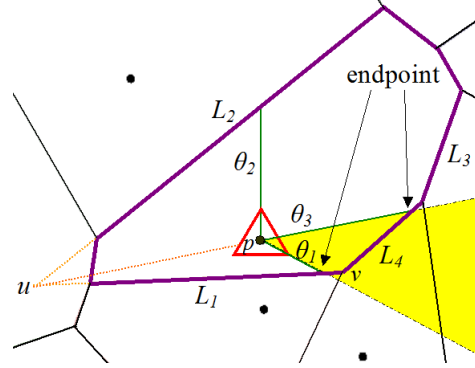


FIGURE 4. Now the cone generated by the subspace  $\{\theta_1, \theta_3\}$  is shown. Since  $v = L_1 \cap L_4$  is a point in the cone and the cell it is a vertex and no further dividing of this cone is needed.

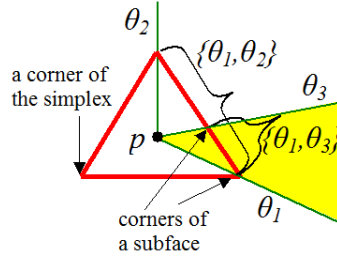


FIGURE 5. The simplex, some of its subfaces, and the conic beam emanating from  $p$  and corresponding to the subspace  $\{\theta_1, \theta_3\}$ .

$T_i = T(\theta_i, p)\theta_i$ ) and finding the corresponding bisecting lines  $L_i$ , we want to use this information for finding all of the possible vertices in the cone generated by the rays. By using equation (3.1) we find the type of intersection between the lines  $L_1, L_2$ . This intersection is either the empty set, a point, or a line.

If (3.1) has no solution of any kind (including solutions which are not non-negative), then the lines  $L_1$  and  $L_2$  are parallel. This is a rare event but it must be taken into account. In this case  $L_1$  and  $L_2$  have the same direction vector  $\phi$ , i.e.,  $L_i = \{q_i + \phi t : t \in \mathbb{R}\}$  for some  $q_i \in \mathbb{R}^2$ ,  $i = 1, 2$  and some unit vector  $\phi$ . We check if the ray emanating from  $p$  in the direction of  $\phi$  is in the cone (happens if and only if the solution  $(\alpha_1, \alpha_2)$  to the linear equation  $\phi = \alpha_1\theta_1 + \alpha_2\theta_2$  is nonnegative). If yes, then we shoot a ray in the direction of  $\theta_3 := \phi$ . Otherwise, we shoot the ray in the direction of  $\theta_3 = -\phi$ . This ray will be contained in the cone and will hit a



---

**Algorithm 1:** The algorithm: a detailed pseudocode

---

```

input : A site  $p$  whose cell is to be computed
output: The vertices and edges of the cell, other information

1 Create the simplex unit vectors;
2 Create the simplex faces and enter them into FaceQueue;
3 while FaceQueue is nonempty do
4   Consider the highest (first) subface in FaceQueue;
5   Denote it by  $\{\theta_1, \theta_2\}$ ;
6   Compute the endpoints  $p + T_i$ ,  $i = 1, 2$ ;
7   Find their neighbor sites  $a_i$ ,  $i = 1, 2$ ;
8   Compute the bisecting line  $L_i$  between  $p$  and  $a_i$ ,  $i = 1, 2$ ;
9   If no such a site  $a_i$  exists, then  $p + T_i$  is on the boundary of the world. Call the
      corresponding boundary line  $L_i$ ;
10  Consider the system of equations (3.1)
11  if  $\det(B) = 0$  then // no solution or  $\infty$  many
12    if  $L_1 = L_2$  then // no vertices here
13      continue;
14    else // parallel lines
15       $\theta_3 = \phi$  where  $\phi$  is the direction vector of the lines;
16      If the ray in the direction of  $\phi$  is not in the cone, then  $\theta_3 = -\phi$ ;
17      Insert the subfaces  $\{\theta_1, \theta_3\}$ ,  $\{\theta_2, \theta_3\}$  into FaceQueue;
18  else //  $\det(B) \neq 0$ , unique solution  $\lambda$ 
19     $u = p + \lambda_1 T_1 + \lambda_2 T_2$ ;
20    if  $\lambda$  is nonnegative then // we're in the cone
21      if  $u$  is inside the cell then
22        Store  $u$ ,  $L_1, L_2$  (and/or neighbor sites;) //  $u$  is a vertex
23      else //  $u$  is outside the cell
24         $\theta_3 = (u - p)/|u - p|$ ;
25        Insert  $\{\theta_1, \theta_3\}$ ,  $\{\theta_2, \theta_3\}$  into FaceQueue;
26      else //  $u$  isn't in the cone
27         $\theta_3 = (p - u)/|p - u|$ ;
28        Insert  $\{\theta_1, \theta_3\}$ ,  $\{\theta_2, \theta_3\}$  into FaceQueue;
29  Remove  $\{\theta_1, \theta_2\}$  from FaceQueue;

```

---

facet of the cell not located on the lines  $L_1$  and  $L_2$  (the facet may be located on the boundary of the bounded world  $X$ ). We divide the current simplex subface using  $\theta_3$  and continue the process.

If  $L_1 = L_2$ , then both endpoints are located on the same line. This corresponds to the case where (3.1) has infinitely many solutions. In this case there is no vertex in the corresponding cone (perhaps one of the endpoints  $p + T_i$  is a vertex, but this vertex will be found later using the neighbor subface). Hence we can finish with the current subface and go to the other ones. Such a case is implicit in Figure 3 when

the rays are shot in the directions of the first and third corners of the simplex and hit  $L_1$ .

If (3.1) has a unique solution  $\lambda = (\lambda_1, \lambda_2)$ , then either it is not nonnegative, i.e., the point  $u = p + \sum_{i=1}^2 \lambda_i T_i$  is not in the cone, or  $\lambda$  is nonnegative, i.e.,  $u$  is in the cone. In the first case the ray emanating from  $p$  in the direction of  $\theta_3 := (p-u)/|p-u|$  will hit an edge of the cell contained in the cone but not located on  $L_1$  or  $L_2$ . Such a case is described in Figure 3 when considering the subface  $\{\theta_1, \theta_2\}$ . We divide the current simplex subface using  $\theta_3$  and continue the process. In the second case  $u$  is in the cone, but we should check whether  $u$  is in the cell (can be checked, for instance, by distance comparisons). If  $u$  is in the cell (corresponding to the case of the subface  $\{\theta_1, \theta_3\}$  in Figure 4, where  $u = v$  there), then it is a vertex and we store it (together with other data: see Section 6). We have finished with the subface and can go to the other ones. Otherwise  $u$  is not a vertex, and we actually found a new edge of the cell corresponding to the ray in the direction of  $\theta_3 := (u-p)/|u-p|$  (implicit in Figure 3 when considering the subface  $\{\theta_2, \theta_3\}$ , i.e., the rays are shot in the directions of the second and third corners of the simplex; in this case  $u$  is the intersection of  $L_1$  and  $L_2$ ). We divide the subface using  $\theta_3$  and continue the process.

From the above description it seems that the method should be implemented in a recursive way. However, by using a simple data structure, one can avoid the need to use a recursive implementation and instead can use loops. The reason that this is possible is because each subface is handled independently of the other subfaces, including its “parent” or “children”: no information is exchanged between the subfaces. As a result, one can maintain a list of subfaces, called *FaceQueue* (each subface is represented by a set of two unit vectors, which correspond to its corners), and run the process until this list is empty. See the pseudocode. The initial list contains the faces of the simplex  $\{\psi_1, \psi_2\}$ ,  $\{\psi_2, \psi_3\}$ ,  $\{\psi_1, \psi_3\}$ , where we can take  $\psi_1 = (\sqrt{3}/2, -1/2)$ ,  $\psi_2 = (0, 1)$ ,  $\psi_3 = (-\sqrt{3}/2, -1/2)$ . In this connection, it should be emphasized that the simplex is used for handling the progress of the algorithm (using the list of subfaces), but the corresponding unit vectors in the direction of the subfaces’ corners are not necessarily on the same line as the one on which the simplex subface is located. Despite this, it is convenient to represent a simplex subface by its associated unit vectors.

## 5. FINDING THE ENDPOINTS EXACTLY

In order to apply Method 3.1, we should be able to find the endpoint  $p + T(\theta_i, p)\theta_i$  emanating from the site  $p$  in the direction of  $\theta_i$  [see (2.1) and line 6 in Algorithm 1]. One possible method is to use the method described in [44], but the problem is that the endpoint found by this method is given up to some error parameter, and unless this parameter is very small (which, in this specific case, implies slower computations), this may cause an accumulating error later when finding the vertices, due to numerical errors in the expressions in (3.1).

In what follows we will describe a new method for finding the endpoint in a given direction  $\theta$  exactly. Of course, when using floating point arithmetic errors appear,

but they are much smaller than the ones described above. See Figure 6 for an illustration.

**Method 5.1.**

- **Input:** A site  $p$  and a unit vector  $\theta$ ;
  - **Output:** the endpoint  $p + T(\theta, p)\theta$ .
- (1) Shoot a ray from  $p$  in the direction of  $\theta$  and stop it at a point  $y$  which is either in the region  $X$  but outside the cell of  $p$ , or it is the intersection of the ray with the boundary of the region. If  $y$  is chosen to be outside the cell, then go to Step (4). Otherwise, let  $L$  be the boundary line on which  $y$  is located;
  - (2) check whether  $y$  is in the cell, e.g., by comparing  $d(y, p)$  to  $d(y, a)$  for any other site  $a$ , possibly with enhancements which allow to reduce the number of distance comparisons;
  - (3) if  $y$  is in the cell, then  $y$  is the endpoint and  $L$  is the bisecting line. The calculation along the ray is complete;
  - (4) otherwise,  $d(y, a) < d(y, p)$  for some site  $a$ . Let  $CloseNeighbor := a$ ;
  - (5) find the point of intersection (call it  $u$ ) between the given ray and the bisecting line  $L$  between  $p$  and  $CloseNeighbor$ . This intersection is always nonempty. The line  $L$  is easily found because it is vertical to the vector  $p - CloseNeighbor$  and passes via the point  $(p + CloseNeighbor)/2$ ;
  - (6) let  $y := u$ ; go to Step (2).

**Remark 5.2.** The correction of this method is quite simple. First, the method terminates after finitely many steps because there are finitely many sites. The point  $u$  in Step (5) is well defined because  $y$  is in the halfspace of  $CloseNeighbor$  and hence the considered ray intersects the boundary  $L$  of this halfspace. The point  $y$  is outputted in Step (3) and by the description of this step  $y$  is in the cell. Since  $y$  is on a bisecting line between  $p$  and another site, and since  $y$  is in the cell, this means that  $y$  must be an endpoint (see (2.1); here  $A = \cup_{j \neq k} \{p_j\}$  and  $T(\theta, p) = |y - p|$ ).

**Remark 5.3.** When finding the endpoint  $y$ , one can also find all of its neighbor sites since in the last time Step (2) is performed, one can easily find all the sites  $a$  satisfying  $d(a, y) = d(p, y)$  simply by storing any site  $a$  satisfying this equality. Call the corresponding list  $EquiDistList$ . Each  $a \in EquiDistList$  induces a corresponding bisecting line  $L$  between  $p$  and  $a$ . In the rare event where  $y$  coincides with a vertex of the cell, there may be  $a \in EquiDistList$  whose bisector  $L$  may not contain a facet of the cell but rather it intersects the cell only at the vertex  $y$  (this can happen only when  $EquiDistList$  has at least 3 different elements, i.e., at least 3 distinct sites located on a circle around  $y$ , and hence this cannot happen when the sites are in general position). This is a problem, since we want to make sure that when we make operations with the endpoint, we use a line  $L$  on which it is located and on which an edge of the cell is located. In order to overcome the problem, one simply needs to know which of the several sites  $a \in EquiDistList$  induces a bisector  $L$  containing an edge of the cell, and then to consider this site and its

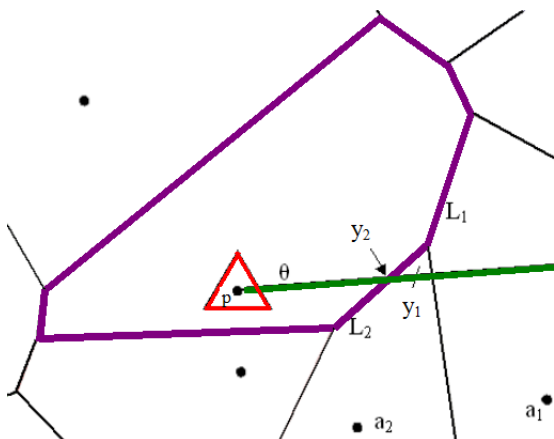


FIGURE 6. Illustration of Method 5.1 for some ray. The ray comes from far away. At the first displayed iteration *CloseNeighbor* is  $a_1$ . The intersection between the corresponding line  $L_1$  and the ray is  $y = y_1$ . At the next stage *CloseNeighbor* is  $a_2$  and  $y = y_2$ . The process terminates since  $y_2$  is in the cell of  $p$ , i.e., it is the endpoint.

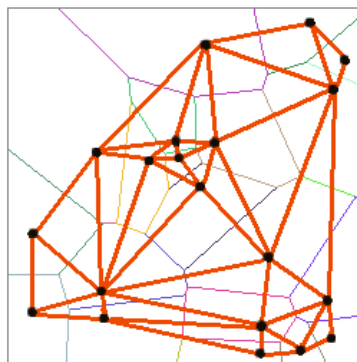


FIGURE 7. The Delaunay graph of 20 sites, restricted to a square in the plane (thick lines). The Voronoi cells of the same sites are shown too (thin lines).

associated line for later operations. This can be easily done by sorting in increasing order all the angles  $\angle pya$ ,  $a \in \text{EquiDistList}$ , or, equivalently, the distances  $d(a, p)$ ,  $a \in \text{EquiDistList}$  (the equivalence is because  $p$  and all the sites  $a \in \text{EquiDistList}$  are on a circle whose center is  $y$ ). The sites corresponding to the two smallest values are the ones which induce a desired bisector.

## 6. STORING THE DATA

In this short section we explain how to the information retrieved by Method 3.1 is stored.

Given a point site  $p = p_k$ , when a vertex  $u$  belonging to the cell of  $p$  is found, one stores the following parameters: its coordinates, the lines from which it was obtained (i.e.,  $u$  belongs exactly to the corresponding facets located on these lines), and the index  $k$ . For storing a line  $L$  it is convenient to store the index of its associated neighbor site, namely the index (simply a number or a label) of the site which induces it (denoted by *CloseNeighbor* in Method 5.1). If it is a boundary line, then it has a unique index number which is stored and from this index one can retrieve the parameters (the normal and the constant) defining the line. Alternatively, these parameters can be stored directly. For some purposes it may be useful to store also some endpoints associated with each line.

A convenient data structure for storing the whole diagram is a one dimensional array, indexed by  $k$ , in which the vertices (represented, as explained above, by coordinates and associated neighbor sites) and any additional information, such as endpoints, are stored. Although the vertices are not stored according to a certain order, it is quite easy to sort them later in clockwise or counterclockwise order by the method of search, e.g., by labeling the rays with corresponding values.

## 7. COMPUTING THE DELAUNAY GRAPH (DELAUNAY TESSELLATION)

Here it is shown how to compute the Delaunay graph of the given sites in an almost automatic way from the data structure used for storing the Voronoi diagrams. This has some value despite the well-known relation between Delaunay graphs and Voronoi diagrams (at least under the assumption that the sites are in general position) because the setting we consider is slightly different, and, in addition, in contrast to familiar procedures, here almost no special computational tasks are required once the data structure used for storing the Voronoi diagram is known.

The Delaunay graph is an important geometric structure which by itself has many applications [6, 22, 41]. By definition, the Delaunay graph consists of vertices and edges. The vertices of the Delaunay graph are the (point) sites. There is an edge between two sites if their Voronoi cells are neighbors (via a face). See Figure 7 for an illustration. Note that here everything is restricted to the given bounded world  $X$ . Rarely it may happen that two sites whose cells are neighbors in the whole plane are not neighbors in  $X$ . This can happen only with cells which intersect the boundary of  $X$ . For overcoming this problem (if one considers this as a problem) one can simply take  $X$  to be large enough or can perform a separate check for the above boundary cells.

As a result, for computing the Delaunay graph one chooses a given site, goes over the data structure used for the Voronoi cells (see Section 6), and finds all the different neighbor sites of a given site. The procedure is repeated for each site and can be easily implemented in parallel. For drawing the Delaunay graph one simply connects two sites by an edge when it is found that one site is a neighbor site to another one.

## 8. HIGHER DIMENSIONS AND A NEW COMBINATORIAL REPRESENTATION FOR THE CELLS

So far it was assumed that setting is the Euclidean plane. However, one may wonder whether it is possible to generalize the ideas and methods to higher dimensions. It turns out that this can be done, at least partly, and this issue is discussed in this section. We also present and discuss a new combinatorial representation for the Voronoi cells (and actually any convex polytope) in higher dimensions, a representation which follows from the discussion given at Section 6.

**8.1. Method 3.1.** The main ideas hold in  $\mathbb{R}^m$  for any dimension  $m \geq 2$ . We simply use a multidimensional simplex instead of a triangle. The system of equations (3.1)

is the same, where now the corresponding vectors become  $m$ -dimensional and  $B$  becomes an  $m$  by  $m$  matrix. The lines  $L_i$  become hyperplanes. The geometric meaning of (3.1) still holds. We note however that because of Step (3), some complications emerge in the actual implementation of this step.

**8.2. Method 5.1.** Generalizes to  $\mathbb{R}^m$  in a complete straightforward way, where now the line  $L$  becomes an hyperplane.

**8.3. Computing the Delaunay graph.** Generalizes to  $\mathbb{R}^m$  in a complete straightforward way.

**8.4. A new combinatorial representation.** As explained in Section 6, each vertex is stored by saving its coordinates and the facets (actually the corresponding neighbor sites which induce these facets) which intersect at the vertex. In dimension  $m = 2$  a vertex  $u$  is always obtained from the intersection of 2 lines. In dimension  $m \geq 3$  a vertex is usually obtained from exactly  $m$  hyperplanes, but in principle it can be obtained from  $S$  hyperplanes,  $S > m$ . We call the set  $\{L_{i_1}, \dots, L_{i_S}\}$  of all the hyperplanes from which  $u$  was obtained the combinatorial representation of  $u$ .

As the examples below show (see also Section 7), once the above combinatorial representation is known and stored, we can obtain other combinatorial information related to the cell, say the neighbors of a given vertex, the  $\ell$ -dimensional faces of some cell, the Delaunay graph, and so on, and hence we do not need to store these types of information separately. This is in contrast to familiar methods for representing the combinatorial information in which one has to find and store all the  $\ell$ -dimensional faces,  $\ell = 0, 1, \dots, m - 1$  of the cell. Since the combinatorial complexity of the cell (the number of multi-dimensional faces) may grow exponentially with the dimension [6, 36], our method may save a lot of space. The price is however that for retrieving some data certain search operations will have to be done on the stored information.

There is another difference between our method and other ones. In other methods one starts with the vertices as the initial (atomic) ingredients, and from them one constructs higher dimensional faces. For instance, an edge is represented by the two vertices which form its corners. However, in our method we start with the highest dimensional faces (located on hyperplanes) and from them we construct the vertices and the other multi-dimensional faces. As a matter of fact, our method of storage can be used to represent any multi-dimensional convex polytope, and even a class of nonconvex or abstract ones.

**Example 8.1.** The possible  $\ell$ -dimensional faces,  $\ell = 0, 1, \dots, m - 1$ , can be found by observing that any such a face is the intersection of hyperplanes. Indeed, the  $(m - 1)$ -dimensional faces are all the hyperplanes  $L_i$  which appear in the representation of the vertices. For finding the  $(m - 2)$ -dimensional faces we fix an hyperplane  $L_i$  and look at all the vertices  $u$  having  $L_i$  in their combinatorial representation. In the representation of any such a vertex  $u$  appear other hyperplanes  $L_j$ , and  $L_i \cap L_j$  is an  $(m - 2)$ -dimensional face. By going over all the possible hyperplanes of  $u$ , all the possible  $u$ , and all the possible  $L_i$ , we can find and represent all the possible  $(m - 2)$ -dimensional faces (for instance,  $L_i \cap L_j$  can be represented by an array

containing the parameters defining both  $L_i$  and  $L_j$ ). A similar procedure can be used for the other  $\ell$ -dimensional faces.

**Example 8.2.** Given a vertex  $u$  with a given combinatorial representation, its neighbor vertices can be found by observing that if  $u$  and  $v$  are neighbors, then they located on the same 1-dimensional face. This face is the intersection of  $m - 1$  hyperplanes. Hence for finding the neighbor vertices of  $u$  we simply need to go over the list of vertices  $v$  and choose the ones whose combinatorial representation contains  $m - 1$  hyperplanes which also appear in the representation of  $u$ .

## 9. SEVERAL THEORETICAL AND PRACTICAL ASPECTS

This section discusses several theoretical and practical aspects related to the algorithm. For the sake of convenience of the reading, the section is divided to a few subsections.

**9.1. A theoretical theorem:** The following theorem describes several aspects related to the algorithm.

**Theorem 9.1.** *Suppose that the world  $X \subset \mathbb{R}^2$  is a compact and convex subset whose boundary is polygonal. Assume also that the distinct point sites  $p_1, \dots, p_n$  are contained in its interior. Then:*

- (a) *Algorithm 1 is correct. More specifically, given any site  $p = p_k$ , the computation of the Voronoi cell of  $p$  by Algorithm 1 terminates after a finite number of steps and the corresponding entries in the output of the algorithm include all the vertices and edges of the cell;*
- (b) *the time complexity, for computing one cell, is bounded above by  $O(r_k e_k)$ , where  $r_k$  is the maximum number of distance comparisons done along each shot ray (compared between all rays in a given cell), and  $e_k$  is the number of edges of the cell;*
- (c) *the time complexity, for the whole diagram, assuming one processing unit is involved, is bounded above (not necessarily tightly) by  $O(n^2)$ ;*
- (d) *the time complexity, for the whole diagram, assuming  $Q$  processing units are involved (independently) and processor  $Q_i$  computes a set  $A_i$  of cells, is*

$$\max\left\{\sum_{k \in A_i} O(r_k e_k) : i \in \{1, \dots, Q\}\right\}.$$

It should be noted that for the time complexity analysis we assume that arithmetic operations, array manipulations, etc., are  $O(1)$  independently of  $n$  (as is the case with the time complexity of many geometric algorithms, including all the Voronoi algorithms we aware of).

**9.2. Ideas behind the proof:** The proof of Theorem 9.1 is quite technical (see Section 10), but the main idea regarding the bound on the time complexity is simple: each time a ray is shot, a new edge of the cell is detected or a vertex is found. This shows (after a careful counting) that the number of rays used for each cell is bounded

by a universal constant times the number of edges in the cell. The operations done along a given ray for detecting its endpoint are mainly distance comparisons (or some  $O(1)$  operations). The maximum number of such operations, compared between all the shot rays, is  $r_k$ , and the upper bound follows. As for the upper bound on the whole diagram, one observes that the total number of edges is of the order of the size of the diagram and recalls the well known fact that this size is  $O(n)$  (see [6, p. 347], [42, pp. 173-5]). Since  $r_k$  is bounded by  $O(n)$  (for each  $k$ ), the bound  $O(n^2)$  follows (see later paragraphs for better estimates under additional assumptions).

**9.3. Serial time complexity: a comparison to other algorithms:** The upper bound on the worst case serial time complexity (one processing unit is involved) is at least as good as the bound  $O(n^2)$  of the incremental method [31], [40], [41, pp. 242-251]. The bound is also better than the corresponding bound of the naive method [41, pp. 230-233] which is  $O(n^2 \log(n))$ . On the other hand, it is worse than the  $O(n \log(n))$  of some algorithms (plan-sweep, divide and conquer, the method based on convex hulls) [6]. It should be emphasized however that it is still not known that the established upper bound is tight (Subsection 9.4), and in addition, even if it is tight, then the main advantage of our algorithm is in its natural ability to support simple parallel computing in various ways (see Subsection 9.6). In addition, in common scenarios (sites which are uniformly distributed) our algorithm behaves more or less in a linear way with respect to the input (Subsection 9.5 below).

**9.4. Serial time complexity: possible improvements:** It is not clear whether the bound on the time complexity presented in Theorem 9.1 is tight, after possibly taking into account several enhancements, but we believe that such enhancements can give better bounds (at least in the one processor case): for example, perhaps by computing the cells in a certain order (e.g., using plan sweep), by improving the endpoint computation (Method 5.1), etc. We do have several experimental results and partial theoretical explanations in the special but important case where the sites are generated by the uniform distribution. If a preprocessing stage (whose complexity is  $O(n)$ ) is performed in which the sites are inserted into a corresponding data structure (buckets) mentioned in [10], then the number of distance comparisons needed for computing the endpoints of the rays can be significantly reduced. In this case the uniform distribution of the sites ensures, with high probability, that only very near sites will be considered for the distance comparisons (the ray will be very short and  $r_k$  will be bounded by  $O(1)$ ). This results in time complexity of  $O(e_k)$  for cell  $k$  and  $O(n)$  for the whole diagram. We also note that under a certain (non-uniform) configuration of sites a given cell can have  $e_k = O(n)$  edges (the remaining cells will have much lower number of edges), but by an efficient search one may bound above  $r_k$  by an estimate better than  $O(n)$ .

**9.5. Serial time complexity: worst case against common scenarios:** The difference between the potential worst case scenarios and the common one is similar in some sense to the Quicksort algorithm for sorting [18, 34] whose average time complexity is  $O(n \log(n))$  but its worst case time complexity is  $O(n^2)$ . The simplex



algorithm for linear programming [20, 21] provides another similar example (efficient in practice, with polynomial time average case complexity [53], but exponential time complexity in the worst case [37]). One can find related phenomena in the Voronoi case, e.g., the average case time complexity  $O(n \log(n))$  of the incremental method [32] against the worst case of  $O(n^2)$ .

**9.6. Parallel time complexity:** So far it was assumed that only one processing unit is involved. If  $Q$  processing units are involved in the computation of the whole diagram, and processor  $Q_i$  computes a set  $A_i$  of cells, then the time complexity is  $\max\{\sum_{k \in A_i} O(r_k e_k) : i \in \{1, \dots, Q\}\}$ . When the sites are uniformly distributed, then with high probability  $O(r_k e_k) = O(1)$  (for instance,  $r_k \leq 50$  and  $e_k \leq 20$ ; for most cells actually  $e_k = 6$ ) and the time complexity becomes  $\max\{O(|A_i|) : i \in \{1, \dots, Q\}\}$ . If all the sets  $A_i$  have the same size  $n/Q$ , then we arrive at the  $O(n/Q)$  time complexity with high probability. This time complexity seems to be the best one available. In the above analysis it was assumed that each cell is computed by a one processing unit. The advantage of our algorithm is that it also allows parallelizing of the computation of each cell, since each subcone can be handled independently of other subcones and so the work can be divided by several processors.

Returning back to the worst case scenario, one may want to avoid cases where a certain large cell slows the whole computation. To avoid this, if a certain processing unit detects a cell having too many sides (e.g., more than 20), then it can halt its work and go to other cells. The sides and vertices of the problematic cell will be found using neighbor cells and will be constructed almost automatically at the end. Alternatively, additional processing units can help to compute the problematic cell.

**9.7. A few words about practical aspects:** It should be emphasized again (see also Section 1) that this paper is theoretical. Despite this, we want to finish this section with a few remarks about some practical issues, or, more precisely, about the current implementation we have. Its actual behavior is somewhat strange: for a reason which is not currently well understood, the running time sometimes grows in a way which is a little bit greater than linear with respect to the input (number of sites) when one processing unit is involved. However, when several processing units are involved, then the running time  $t(n)$  is better than linear with respect to the input (i.e.,  $t(\alpha n) < \alpha t(n)$  for any tested  $\alpha \in \mathbb{N}$ ; this does not contradict the obvious lower bound of  $O(n)$ ). Perhaps (in both cases) this may be related to something in the memory management or some influence of the operating system.

Comparing to well-known implementations, our preliminary implementation performs quite good. For example, it runs faster than Qhull 2011.1 [9] when a Voronoi diagram of  $10^6$  sites is computed (a few seconds on a standard computer). However, it does not run faster than Triangle [51, 52]. Both Qhull and Triangle are veteran serial implementations (more than 16 years) which have adopted many enhancements over the years. Despite this, their behavior is worse than linear and their output is not always correct. In contrast, in our implementation only two people have been

involved (only one of them has done the programming work) and many enhancements are waiting to be implemented. For instance, each vertex usually belongs to 3 cells and hence it is computed 3 times, while in Qhull/Triangle it is computed only once. In addition, at least in the multiprocessor case, it is better than linear, and so far no incorrect output has been observed when double precision arithmetic was used. A detailed description of experimental results and more details about implementation issues in various environments will be discussed elsewhere.

## 10. PROOF OF THEOREM 9.1

In this section we prove Theorem 9.1 which shows the correction of the algorithm and presents an upper bound on its time complexity. The proof is based on several lemmas. Here are additional details regarding notation and terminology. In the sequel  $p = p_k$  is a given site. We assume that the sites are different, and hence we have  $\min\{d(p_k, p_j) : k \neq j\} > 0$ . Since the distance between  $p$  and the boundary of the cell is positive, there is a small circle with center  $p$  which is contained in the interior of the cell. On this circle we construct the simplex, which, as a consequence, has a positive distance from the boundary of the cell and from  $p$ . Any other simplex which may be used in the algorithm for producing the rays and detecting the vertices is simply a scalar multiplication of this small simplex and it produces exactly the same rays (hence enables to detect the same vertices). Recall again that we use the notion “face” or “facet” for denoting an edge of the cell (a side).

A vertex  $v$  of the cell is said to correspond to a subface  $F$  of the simplex if  $v$  is located inside the cone corresponding to  $F$ . For instance, in Figure 4 the vertex  $v$  corresponds to the subface  $F = \{\theta_1, \theta_3\}$  and no other vertices correspond to  $F$ . All the rays we consider emanate from a given site  $p = p_k$  and are sometimes identified with their direction vectors. Given a cone generated by two rays, the rays on the boundary of the cone are called boundary rays and any other ray in the cone is called an intermediate ray. For instance, in Figure 4 if we look at the cone generated by  $\theta_1$  and  $\theta_2$ , then these rays are boundary rays and  $\theta_3$  is an intermediate ray. Continuing with Figure 4, after additional steps additional rays will be generated between  $\theta_1$  and  $\theta_3$ , and hence they will be intermediate rays in the cone generated by  $\theta_1$  and  $\theta_2$  (and also of the one generated by  $\theta_1$  and  $\theta_3$ ). Between  $\theta_1$  and  $\theta_3$  no additional rays will be generated.

Part of the proof is to analyze the time complexity of the algorithm and in particular to prove that the algorithm terminates after finitely many steps. For doing this it is convenient to consider the algorithm tree, namely the graph whose nodes are the main stages in the algorithm, and a node has subnodes (children nodes) whenever a conditional operation (separating into cases, if-else, etc.) is made in the node whose result is a non-terminating-condition statement (i.e., further work is required by the algorithm to achieve a terminating condition). Once we are given an upper bound on the number of nodes in the tree and on the number of operations done in each node, we have an upper bound on the time complexity of the algorithm. See Figure 8 for an illustration of the algorithm tree for the cell described in Figure 3.

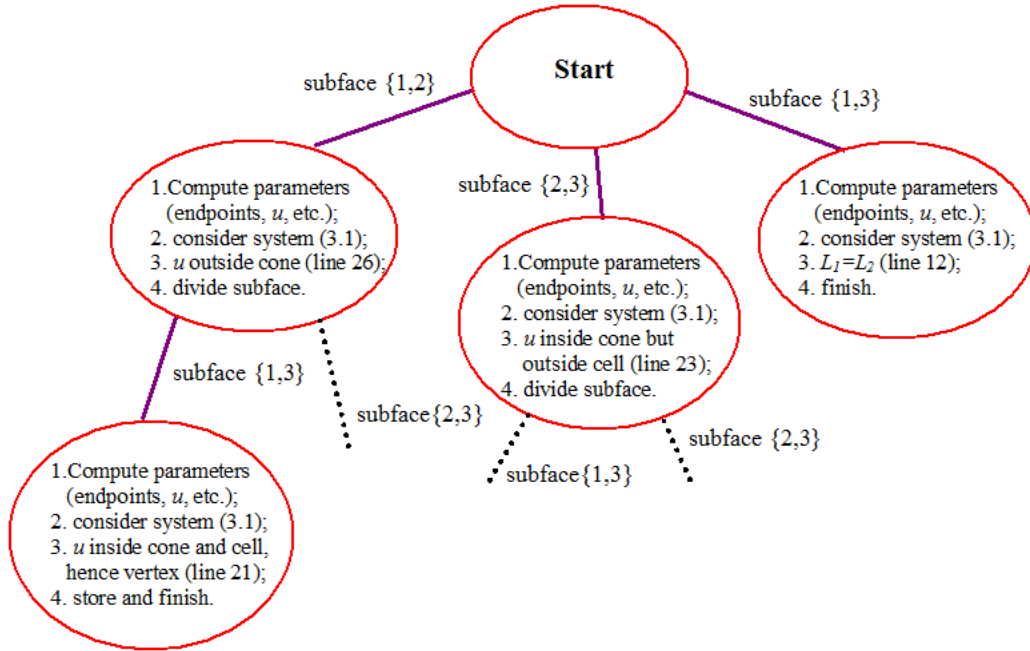


FIGURE 8. Illustration of the algorithm tree for the cell of Figure 3.

In Algorithm 1 there are two types of nodes: in the first type (lines 12 and 21) the algorithm finishes its consideration with the current subface (perhaps after storing some information) without further dividing it. In the second type (lines 14, 23, and 26) the subface is divided into two subfaces and the algorithm continues with both of them. In other words, in the first type there are no children nodes and in the second one there are. For the sake of simpler analysis, the computation of the two endpoints done in line 6 (or passing them in a computed form from previous stages), a computation which is done before each conditional operation, is considered as performed in each node and not in a separated node. If, for the sake of fully counting the number of nodes, such a computation is considered in a separate node, then the total number of nodes will be greater by at most a factor of 2 than in our analysis since before each of the two types of nodes mentioned above there is only one “endpoint computation node”.

**Lemma 10.1.** *Consider a simplex subface  $F = \{\theta_1, \theta_2\}$  and the corresponding cone generated from it. Let  $L_1$  and  $L_2$  be the lines on which the endpoints  $p + T(\theta_i, p)\theta_i$ ,  $i = 1, 2$  are located. Suppose that an intermediate ray in the direction of  $\theta_3$  is generated when  $F$  is considered. Then the ray of  $\theta_3$  hits a facet different from  $\widetilde{L}_i, i = 1, 2$ .*

*Proof.* First note any ray generated by the algorithm does hit a facet  $\widetilde{L}_3$ . Indeed, the ray starts at a point inside the cell and goes outside the cell, possibly outside

the region  $X$  (because  $X$  is bounded). Thus the intermediate value theorem implies that this ray intersects the boundary of the cell, namely, a certain facet  $\widetilde{L}_3$  (the point hit by the ray is  $p + t\theta$  where  $\theta$  is a unit vector in the direction of the ray and  $t = \sup\{s \in [0, \infty) : p + s\theta \text{ in the cell}\}$ ).

Denote by  $g$  the point hit by the ray. This point is in fact the endpoint. Indeed, by the definition of the endpoint (see (2.1)) the ray of  $\theta_3$  has an endpoint  $p + T(\theta_3, p)\theta_3$ . Any point on the ray after  $g$  is strictly outside the cell (either because it is outside the world or because it is in a halfspace of another site). Thus  $p + T(\theta_3, p)\theta_3 \in [p, g]$ . However, any point beyond  $[p, p + T(\theta_3)\theta_3]$  is outside the cell by the definition of the endpoint. Since we know that  $g$  is in the cell (it belongs to the facet  $\widetilde{L}_3$ ) we obtain that  $g \in [p, p + T(\theta_3)\theta_3]$ . Thus  $g = p + T(\theta_3, p)\theta_3$ .

Now we observe that an intermediate ray is created only when either  $L_1$  and  $L_2$  are parallel (line 14), or when they intersect in the cone but outside the cell (line 23), or when they intersect outside the cone (line 26).

In the first case the line on which the ray of  $\theta_3$  is located is parallel to  $L_1$  and  $L_2$ , and hence cannot hit them. In particular  $\widetilde{L}_3 \neq \widetilde{L}_i, i = 1, 2$ .

Now consider the second case and suppose for a contradiction that, say,  $\widetilde{L}_1 = \widetilde{L}_3$ . Let  $u = L_1 \cap L_2$ . By assumption  $u$  is outside the cell. In particular  $u$  is hit by the ray of  $\theta_3$  (see line 23) and  $u \neq p + T(\theta_3, p)\theta_3$ . But both  $u$  and  $p + T(\theta_3, p)\theta_3$  are assumed to belong to  $\widetilde{L}_1$  and hence to  $L_1$ . Since a line is fully determined by two distinct points on it,  $L_1$  contains the ray of  $\theta_3$  and in particular passes via  $p$ . This is impossible since  $p$  is in the interior of the cell and hence its distance to any of the boundary lines is positive.

Now consider the third case and suppose for a contradiction that, say,  $\widetilde{L}_1 = \widetilde{L}_3$ . Let  $u = L_1 \cap L_2$ . By assumption  $u$  is outside the cone generated by the rays of  $\theta_1$  and  $\theta_2$ . Since  $\theta_3$  is in the direction of  $p - u$  (see line 27), it does not hit  $u$  and hence  $u \neq p + T(\theta_3, p)\theta_3$ . But both  $u$  and  $p + T(\theta_3, p)\theta_3$  are assumed to belong to  $\widetilde{L}_1$  and hence to  $L_1$ . Since a line is fully determined by two distinct points on it,  $L_1$  contains the segment  $[u, p + T(\theta_3, p)\theta_3]$  and in particular it passes via  $p$ . This is impossible since  $p$  is in the interior of the cell and hence its distance to any of the boundary lines is positive.  $\square$

**Lemma 10.2.** *Consider two different rays generated by the algorithm, say in the direction of  $\phi_1$  and  $\phi_2$ . These rays may belong to different simplex subfaces but both of them are assumed to be between (and possibly coincide with) two initial rays, i.e., rays induced by two corners of the simplex. Consider an intermediate ray between the rays of  $\phi_i, i = 1, 2$  whose direction vector is  $\theta_3$ . Then the endpoint of the ray of  $\theta_3$  and the endpoints of the rays of  $\phi_1$  and  $\phi_2$  must be located on different facets.*

*Proof.* Suppose to the contrary that this is not true, say the endpoint of the ray of  $\phi_1$  and the endpoint of the ray of  $\theta_3$  are located on the same facet  $\widetilde{L}$ . Because the ray of  $\theta_3$  is between two initial rays it is generated from some subface  $\{\theta_1, \theta_2\}$ . Here  $\theta_1$  is between  $\psi_1$  and  $\theta_3$  and possibly equals  $\phi_1$ , and  $\theta_2$  is between  $\theta_3$  and  $\phi_2$  and possibly equals  $\phi_2$ . This generation corresponds to the routines of lines 14, 26, or

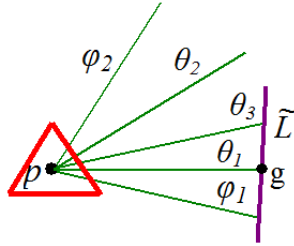


FIGURE 9. An illustration of Lemma 10.2.

23 of the algorithm and in particular  $\theta_1 \neq \theta_3$  and  $\theta_2 \neq \theta_3$ . Denote by  $\tilde{L}_i$ ,  $i = 1, 2$  the facets on which the endpoints corresponding to  $\theta_i$ ,  $i = 1, 2$  are located.

The ray of  $\theta_1$  intersects  $\tilde{L}$  at some point  $g$  which is its endpoint as explained in the proof of Lemma 10.1. See also Figure 9. We conclude that the endpoints of the rays of  $\theta_3$  and of  $\theta_1$  are located on the same facet. But this is impossible, since by assumption  $\theta_3$  was created from the simplex subface  $\{\theta_1, \theta_2\}$  and as already mentioned, this can happen only when either  $L_1$  and  $L_2$  are parallel (line 14), or when they intersect outside the cone (line 26) or when they intersect in the cone but outside the cell (line 23), and in all of these cases the ray of  $\theta_3$  hits a facet different from the ones associated with  $\theta_1$  and  $\theta_2$  (see Lemma 10.1). We arrived at a contradiction which proves the assertion.  $\square$

**Lemma 10.3.** *The algorithm terminates after a finite number of steps. In particular, the number of intermediate rays is finite.*

*Proof.* This follows from Lemma 10.2. Indeed, suppose for a contradiction that the algorithm does not terminate after finitely many steps. This means that the list of simplex subfaces *FaceQueue* is never empty. But in each stage of the algorithm (each node), either a subface is divided (lines 14, 23, and 26) and then replaced by its children subfaces and deleted from *FaceQueue*, or it has no children subfaces (lines 12 and 21) and hence it is deleted from *FaceQueue* shortly after its creation. After a subface is deleted from *FaceQueue* it is never created again. As a result, the fact that the algorithm does not terminate after finitely many steps implies that we can find an infinite sequence of nested distinct subfaces. When a subface is created a new edge of the cell is detected (because of Lemma 10.2) and such an edge could not be detected before, again because of Lemma 10.2. Thus infinitely many distinct edges are detected, contradicting the fact that each cell has only finitely many edges. Hence the algorithm terminates after finitely many steps and in particular finitely many intermediate rays are created.  $\square$

**Lemma 10.4.** *Given a cone generated by two distinct unit vectors  $\theta_1$  and  $\theta_2$  (located between initial rays), let  $E$  be the number of facets of the cell hit by intermediate rays, i.e., rays produced by the algorithm inside the cone excluding the boundary*

rays of the cone. Then the tree of the restriction of the algorithm to the given cone contains exactly  $2E + 1$  nodes.

*Proof.* The proof is by induction on  $E$ . By Lemma 10.3 we know that  $E$  is finite. Let  $L_i$  be the facet on which the endpoint  $p + T(\theta_i, p)\theta_i$  is located,  $i = 1, 2$ . If  $E = 0$ , then there are two cases. In the first case the rays generated by  $\theta_i$ ,  $i = 1, 2$  hit the same facet and in this case (line 12) the current simplex subface is deleted from *FaceQueue*. Thus no subnode of the current node is created, i.e., the restriction of the algorithm tree to the cone contains  $1 = 2E + 1$  nodes. In the second case the rays must hit different facets which intersect at a vertex, since otherwise either no intersection occurs or the intersection is a point outside the cell or outside the cone, and the corresponding ray in the direction of  $\theta_3$  (lines 14, 23, 26) hits a facet contained in the cone, contradicting  $E = 0$ . Therefore also in this case the current subface is deleted from *FaceQueue* and no subnode of the current node is created and the restriction of the algorithm tree to the cone contains  $2E + 1 = 1$  nodes.

Now assume that the claim holds for any nonnegative integer not exceeding  $E - 1 \geq 0$ . It will be proved that it holds for  $E$  too. Indeed, if the current simplex subface  $\{\theta_1, \theta_2\}$  is not divided into two subfaces  $\{\theta_1, \theta_3\}$  and  $\{\theta_2, \theta_3\}$ , then the restriction of the algorithm tree to the cone generated by  $\{\theta_1, \theta_2\}$  contains only one node and hence there cannot be any facet different from  $\widetilde{L}_1$  and  $\widetilde{L}_2$  which is hit by rays produced by the algorithm, contradicting the assumption that  $E \geq 1$ . Knowing that  $\{\theta_1, \theta_2\}$  is divided, i.e., the root node has 2 children, consider the number of facets  $e_{1,3}$  and  $e_{2,3}$  of the cell contained in the cones generated by  $\{\theta_1, \theta_3\}$  and  $\{\theta_2, \theta_3\}$  respectively, excluding, in each cone, the facets (1 or 2) hit by the boundary rays. Since  $E = e_{1,3} + e_{2,3} + 1$  (where the 1 comes from the facet hit by the ray in the direction of  $\theta_3$ ) it follows that  $e_{1,3} < E$  and  $e_{2,3} < E$ . Thus the induction hypothesis implies that the trees of the restriction of the algorithm to the cones generated by the subfaces  $\{\theta_1, \theta_3\}$  and  $\{\theta_2, \theta_3\}$  contain exactly  $2e_{1,3} + 1$  and  $2e_{2,3} + 1$  nodes, respectively. Hence the tree generated by the restriction of the algorithm to the original cone (the one corresponding to  $\{\theta_1, \theta_2\}$ ) contains  $(1 + 2e_{1,3}) + (1 + 2e_{2,3}) + 1 = 2E + 1$  nodes, as claimed.  $\square$

**Lemma 10.5.** *Given a cell of some site  $p = p_k$ , the restriction of the algorithm tree to this cell contains at most  $2e_k - 1$  nodes, where  $e_k$  is the number of facets of the cell.*

*Proof.* Consider the 3 cones generated by the very initial rays, i.e., the rays shot in the direction of the corners of the simplex. The number of nodes in the algorithm tree restricted to the cell is the sum of nodes in each of the trees corresponding to the above cones. By Lemma 10.4 we conclude that this number is  $2(E_{1,2} + E_{2,3} + E_{1,3}) + 3$ , where  $E_{i,j}$ ,  $i \neq j$ ,  $i, j \in \{1, 2, 3\}$  are the number of facets hit by intermediate rays.

Note that a facet  $\widetilde{L}$  cannot be hit by two intermediate rays belonging to two different initial cones. Indeed, assume to the contrary that this happens, say  $\theta_{1,2}$  is the direction of an intermediate ray belonging to an initial cone generated by  $\theta_1$  and  $\theta_2$ , and  $\theta_{2,3}$  is the direction of an intermediate ray belonging to an initial cone

generated  $\theta_2$  and  $\theta_3$ . These two intermediate rays cannot be opposite, otherwise  $\tilde{L}$  will be parallel to itself (without coinciding with itself). Hence  $\theta_2$  is (strictly) in the linear cone generated by  $\theta_{1,2}$  and  $\theta_{2,3}$ , that is  $\theta_2 = \lambda_{1,2}\theta_{1,2} + \lambda_{2,3}\theta_{2,3}$  for some  $\lambda_{1,2} > 0$  and  $\lambda_{2,3} > 0$ . The part of the facet  $\tilde{L}$  between the endpoints of the cone is the convex combination of them, i.e., the segment  $[p + T(\theta_{1,2}, p)\theta_{1,2}, p + T(\theta_{2,3}, p)\theta_{2,3}]$ .

A direct calculation shows that the ray of  $\theta_2$  intersects  $\tilde{L}$  at a unique point  $g$ : this is done by proving that there exist unique  $t$  and  $\alpha \in (0, 1)$  satisfying

$$p + t\lambda_{1,2}\theta_{1,2} + t\lambda_{2,3}\theta_{2,3} = \alpha(p + T(\theta_{1,2}, p)\theta_{1,2}) + (1 - \alpha)(p + T(\theta_{2,3}, p)\theta_{2,3}) \quad (10.1)$$

by equating the corresponding coefficients. The point  $g$  belongs to the cell and hence it is located on the ray of  $\theta_2$  prior to the endpoint  $p + T(\theta_2, p)\theta_2$ . But any point on the ray after  $g$  is outside the cell since it is located either outside  $X$  (if  $\tilde{L}$  is a boundary edge of  $X$ ) or in a halfspace of a different site. Thus  $g = p + T(\theta_2, p)\theta_2$ . This contradicts Lemma 10.2 which implies that the endpoint corresponding to  $\theta_2$  is located on a facet different from the ones corresponding to  $\theta_{1,2}$  and  $\theta_{2,3}$ , i.e., different from  $\tilde{L}$ . We arrived at a contradiction which proves the assertion.

From the previous two paragraphs we can conclude that  $E_{1,2} + E_{2,3} + E_{1,3} \leq e_k$ . However, in fact we can conclude that  $E_{1,2} + E_{2,3} + E_{1,3} \leq e_k - 2$  because the set of facets of the cell is the disjoint union of the set of facets hit by intermediate rays and the facets hit by the three initial rays, and this latter set contains at least two different facets. The assertion follows.  $\square$

**Lemma 10.6.** *Consider the tree generated by the algorithm for the whole diagram. The number of nodes in this tree is bounded by  $O(n)$ .*

*Proof.* The algorithm tree for the whole diagram is the union of the trees corresponding to each cell and an additional root node. By Lemma 10.5 the tree of the cell of  $p_k$  has at most  $2e_k - 1$  nodes, where  $e_k$  is the number of facets of the cell. The set of facets of each cell can be written as the disjoint union of two sets: the set of facets located on the boundary of the polygonal world  $X$  and the set of facets located on a bisecting line between  $p_k$  and another site  $p_j$ ,  $j \neq k$ . The size  $w_k$  of the first set is not greater than the number of facets of  $X$ . In fact, we have  $\sum_{k=1}^n w_k \leq |X| = O(1)$  where  $|X|$  is the number of facets of  $X$ . Denote by  $b_k$  the size of the second set. It is well known that  $\sum_{k=1}^n b_k = O(n)$  (see, e.g., [6, p. 347], [42, pp. 173-5]; in [6] it is assumed that the sites are in general position; however, if this is not true, then a small perturbation of them to a general position configuration actually enlarges the number of facets as explained in [42]). Therefore  $\sum_{k=1}^n e_k = \sum_{k=1}^n w_k + \sum_{k=1}^n b_k = O(n)$  and the total number of nodes in the algorithm tree of the diagram is bounded by  $O(n)$ .  $\square$

**Lemma 10.7.** *The number of calculations needed to find the endpoint in some given direction, using Method 5.1, is bounded by a linear expression of  $n$  (but see also the final paragraph)*

*Proof.* As in previous lemmas, one can build the algorithm tree for Method 5.1 (see also Figure 6). Each node is a place where it is checked whether the temporary

endpoint  $y$  is in the cell (using distance comparisons). If yes, then the algorithm terminates, and if not, then  $y$  is further gets closer to the given site  $p = p_k$ . The obtained tree is linear. Whenever a distance comparison is made with some site  $a = p_j, j \neq k$  (or even with  $p$  itself) and it is found that  $d(y, p) \leq d(y, a)$ , then there is no need to consider this site in later distance comparisons since the previous inequality means that  $y$  is in the halfspace of  $p$  (with respect to  $a$ ) and because  $y$  always remains on the same ray and gets closer to  $p$ , it remains in this halfspace, i.e., also later temporary endpoints  $y$  will satisfy  $d(y, p) \leq d(y, a)$ . However, even if  $d(a, p) < d(a, y)$  then  $a$  should not be considered anymore, since this case implies that  $y$  will be moved to the intersection between its ray and the bisecting line between  $p$  and  $a$ , and so in the next iterations it will satisfy  $d(y, p) \leq d(y, a)$ .

It follows that the total number of distance comparisons is no greater than  $n$ . A simple way to perform the above operation of not considering a given site anymore is to go over the array of sites by incrementing an index starting from the first site. By doing this each site will be accessed exactly one time and when the index will arrive to the end, the process will end. Hence the number of nodes is  $O(n)$ . Each calculation done in a given node is either an arithmetic operation, array manipulations, etc., i.e., it is  $O(1)$ , or it involves a distance comparison (each comparison is  $O(1)$ ). Hence the total number of calculation is  $O(n)$  and the assertion follows.

As a final remark, we note that in practice, not considering a given site anymore can be applied by using more efficient methods than the one described above for reducing the number of calculations and they actually lead to  $O(1)$  operations with high probability whenever the sites are generated using the uniform distribution (see Section 9 Subsection 9.4).  $\square$

**Lemma 10.8.** *The time complexity for computing the cell of  $p_k$  is bounded above by  $O(r_k e_k)$ , where  $r_k$  is the maximum number of distance comparisons done along each shot ray (compared between all shot rays), and  $e_k$  is the number of edges of the cell.*

*Proof.* Lemma 10.5 implies that the size of the algorithm tree restricted to the cell of  $p_k$  contains at most  $2e_k - 1 = O(e_k)$  nodes. The calculations done in each node are either calculations done when a ray is shot (for computing its endpoint) or some  $O(1)$  calculations, when there is no need to compute a new endpoint (since the considered endpoints are already known) and only arithmetic operations, array manipulations, etc., are done. When an endpoint is computed, some operations are done along the corresponding ray. These operations are either distance comparisons or some related  $O(1)$  operations (arithmetic operations, etc.: see the proof of Lemma 10.7). Hence the number of operations is linear in the number of distance comparisons and hence the maximum number of these operations, compared between all the shot rays, is  $O(r_k)$ . The upper bound  $O(r_k e_k)$  follows.  $\square$

**Lemma 10.9.** *The time complexity, for the whole diagram, assuming  $Q$  processing units are involved (independently) and processor  $Q_i$  computes a set  $A_i$  of cells, is  $\max\{\sum_{k \in A_i} O(r_k e_k) : i \in \{1, \dots, Q\}\}$ .*



*Proof.* This is a simple consequence of Lemma 10.8 because the processing units do not interact with each other and the cumulative time for computing a set of cells is the sum of times for computing each cell separately.  $\square$

**Lemma 10.10.** *The time complexity of the algorithm for the whole diagram, when one processing unit is involved, is bounded above by  $O(n^2)$ .*

*Proof.* By Lemma 10.6 the time complexity of the algorithm for cell  $k$  is bounded by  $O(r_k e_k)$ . Since  $r_k \leq n$  and  $\sum_{k=1}^n e_k = O(n)$  (see the proofs of Lemma 10.7 and Lemma 10.6 respectively), the bound  $O(n^2)$  follows. Alternatively, one can obtain the same bound using these lemmas directly (without referring to their proofs) since the number of nodes in the algorithm tree of the whole diagram is  $O(n)$  and the number of calculations done in each node is bounded by  $O(n)$ .  $\square$

In the remaining part of this section we prove the correctness of the output of the algorithm.

**Lemma 10.11.** *Let  $F = \{\theta_1, \theta_2\}$  be a subface of the simplex and let  $p + T(\theta_i, p)\theta_i$ ,  $i = 1, 2$  be the corresponding endpoints.*

- (a) *If both endpoints are on the same facet, then the only possible vertices corresponding to  $F$  are the endpoints.*
- (b) *If one endpoint is on one facet and the other is on another one, and both facets intersect at some vertex  $v$  of the cell, then the only possible vertices corresponding to  $F$  are the endpoints and  $v$ .*

*Proof.* We first prove Part (a). This part seems quite obvious, but it turns out that a complete proof taking into account all the details requires some work. For an illustration, see Figure 10. Let  $T_i = T(\theta_i, p)\theta_i$ ,  $i = 1, 2$ . By assumption, both endpoints  $p + T_i$ ,  $i = 1, 2$  are on some facet  $\tilde{L}$  of the cell. The segment  $[p + T_1, p + T_2]$  is contained in  $\tilde{L}$  since  $\tilde{L}$  is convex. Suppose by way of contradiction that  $v$  is a vertex corresponding to  $F$  which is not one of the endpoints  $p + T_1, p + T_2$ . Then  $v$  is strictly in the cone generated by the endpoints, that is,  $v = p + \lambda_1 T_1 + \lambda_2 T_2$  for some  $\lambda_1, \lambda_2 \in (0, \infty)$ . A simple calculation (similar to that of (10.1)) shows that the ray emanating from  $p$  in direction  $v - p$  intersects the segment  $[p + T_1, p + T_2]$  in exactly one point  $w$ . It must be that  $w = v$ , since the part of the ray beyond  $w$  is strictly outside the cell of  $p$ , the part of the ray prior to  $w$  is strictly inside the cell, and  $v$  is in the cell and it is a boundary point. As a result,  $v \in [p + T_1, p + T_2] \subseteq \tilde{L}$ . Since  $v$  is a vertex of the cell, it must belong to another facet  $\tilde{M}$ .

Let  $v' \neq v$  be some point in  $\tilde{M}$ . Then  $v'$  cannot be on the line  $L$  on which  $\tilde{L}$  is located, since in this case  $\tilde{L} \cap \tilde{M}$  will include a non-degenerate interval (the interval  $[v, v']$ ), a contradiction to the fact that two different facets intersect at a point or do not intersect at all. In addition,  $v'$  cannot be in the half-plane generated by  $L$  in which  $p$  is located. Indeed, suppose to the contrary that this happens (see Figure 10). First note that  $v'$  is not on the ray emanating from  $v$  and passing via  $p$  because this means that  $[v, v']$ , but this is impossible because  $p$  is an interior point. Indeed, a well known fact [46, Theorem 6.1, p. 45] says that because the underlying subset

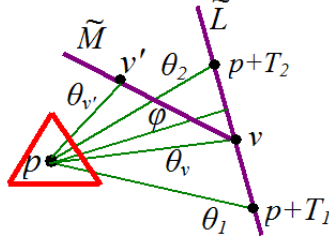


FIGURE 10. An illustration of one of the cases described in Lemma 10.11(a).

(the Voronoi cell in our case) is convex and because  $p$  is in its interior and  $v$  belongs to it, the half open segment  $[p, v)$  is contained in the interior of the cell. Thus  $v'$  is in the interior of the cell, a contradiction. Consider now the cone generated by the rays emanating from  $p$  and passing via  $v$  and  $v'$ . Denote  $\theta_v = (v - p)/|v - p|$  and  $\theta_{v'} = (v' - p)/|v' - p|$ . Any ray  $\phi$  between  $\theta_v$  and  $\theta_{v'}$  close enough to  $\theta_v$  (i.e., its generating unit vector is close enough to  $\theta_v$ ) intersects the segment  $[v', v) \subset \tilde{M}$ , and later it intersects  $\tilde{L}$  as a simple calculation shows (using the fact that  $v$  is in the open segment  $(p + T_1, p + T_2)$  and the assumption on  $v'$ ). However, once a ray emanating from  $p$  intersects a facet of the cell, then this point is its endpoint, namely, its remaining part beyond the point of intersection is outside the cell. Hence the point of intersection of the ray of  $\phi$  with  $\tilde{L}$  is outside the cell, contradicting the fact that it is on  $\tilde{L}$  and hence it is in the cell.

As a result, the only possibility for  $v'$  is to be in the other half-plane generated by  $L$ , a contradiction to the fact that any point in this half-space is outside the cell. This contradiction completes the proof of part (a).

Now consider Part (b). Let  $\theta_3 = (v - p)/|v - p|$ , and let  $F_1 = \{\theta_1, \theta_3\}$  and  $F_2 = \{\theta_2, \theta_3\}$ . The possible vertices corresponding to  $F$  are the unions of the ones corresponding to  $F_1$  and  $F_2$ . Because  $v$  belongs to two different facets it follows that  $p + T_i$ ,  $i = 1, 3$  are on one facet, and  $p + T_i$ ,  $i = 2, 3$  are on another facet. By Part (a) the only possible vertices corresponding to  $F_1$  and  $F_2$  are their corresponding endpoints  $p + T_i$ ,  $i = 1, 2, 3$ , i.e., the endpoints corresponding to  $F$  and the vertex  $v$ .  $\square$

**Lemma 10.12.** *The stored points are vertices of the cell of  $p$ .*

*Proof.* This is evident, since each such a point  $u$  is inside the cell and it is the intersection of two edges of the cell (line 22 of Algorithm 1).  $\square$

In the following lemmas we use the concept of a “prime subspace”, namely a subspace created by the algorithm at some stage but which has not been further divided after its creation. Because of Lemma 10.3 there are finitely many prime subspaces. Any two such subspaces either do not intersect or intersect at exactly one point (their corner), and their union is the simplex around  $p$ . See Figure 11 for an illustration.

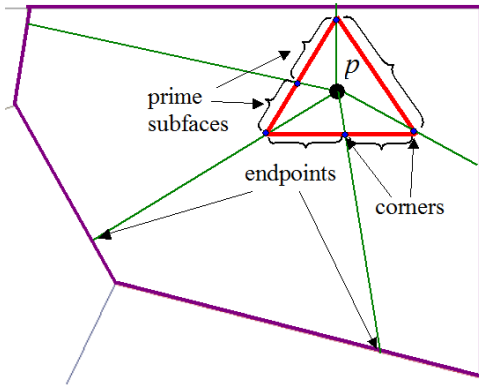


FIGURE 11. Prime subfaces and their rays.

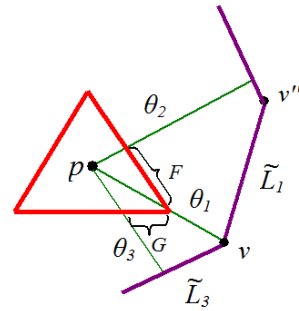


FIGURE 12. Illustration of Lemma 10.13.

**Lemma 10.13.** *Let  $v$  be a vertex of the cell and assume that it coincides with an endpoint corresponding to a corner of a prime subface  $F$ . Then  $v$ , as a vertex, is found and stored by the algorithm.*

*Proof.* The proof is not immediate as it may perhaps seem at first, since a vertex is found by the algorithm only after an intersection between two facets of the cell is detected, and so although  $v$  was found, as an endpoint, it is still not known that it is a vertex, and further calculations are needed in order to classify it as a vertex. Such a problematic situation mainly occurs at the routine of line 12 (the endpoints of a given subface are on the same facets), because even if one of the endpoints is a vertex, it is not stored. Hence this vertex must be detected (and stored) when considering another subface.

Assume by way of contradiction that  $v$ , as a vertex, is not found. Let  $p + T_1$  and  $p + T_2$  be the endpoints corresponding to the corners of  $F$ . Let  $\tilde{L}_1, \tilde{L}_2$  be the corresponding facets of the cell on which these endpoints are located. The facets  $\tilde{L}_i, i = 1, 2$  are located on corresponding lines  $L_1, L_2$ . By assumption  $v$  coincides with one of the endpoints, say with  $p + T_1$ . See Figure 12.

Since  $p + T_1$  corresponds to a corner of  $F$ , this corner is located on another prime subface  $G$ . Therefore  $v$  is also in the cone corresponding to  $G$ . Let  $T_3 = T(\theta_3, p)\theta_3$ . Let  $p + T_3$  be the other endpoint corresponding to  $G$ . It is located on some facet  $\tilde{L}_3$  of the cell. Consider the lines  $L_1$  and  $L_3$  corresponding to  $\tilde{L}_1$  and  $\tilde{L}_3$  respectively. If they do not intersect, or intersect at a point outside the cone corresponding to  $G$  or inside the cone but outside the cell, then by the definition of the algorithm  $G$  must be divided, a contradiction ( $G$  is assumed to be prime). Note also that the equality  $\tilde{L}_3 = \tilde{L}_1$  is impossible because it will imply that  $v$  is in the interior of the facet  $\tilde{L}_1$  and this cannot happen to a vertex. Hence  $L_1 \neq L_3$  and it follows that  $L_1$  and  $L_3$  intersect at a point  $v_{13}$  which is in the cone and in the cell, i.e., a vertex.

A basic property of the polygonal boundary is that any facet of the cell intersects exactly two additional facets. In particular this is true for  $\tilde{L}_1$ : one intersection occurs

at the vertex  $v$  and another one at another vertex  $v''$  located on  $\widetilde{L}_1$  in the direction (along  $\widetilde{L}_1$ ) from  $v$  to  $p + T_2$ . Consider the line passing via  $p$  and  $v$ : it separates the plane into two halfplanes. One of them contains the ray  $\theta_2$  and actually  $\widetilde{L}_1$  (and hence also  $v''$ ). The other contains the ray  $\theta_3$  (and intersects  $\widetilde{L}_1$  only at  $v$ ) and hence also the facet  $\widetilde{L}_3$ . Thus  $\widetilde{L}_3$  cannot intersect  $\widetilde{L}_1$  at the halfplane of  $v''$ . Since we know that  $\widetilde{L}_3$  intersects  $\widetilde{L}_1$  this can only be at  $v$ . Hence  $v_{13} = v$  but since  $v_{13}$  is a vertex, this means that  $v$  is found as a vertex when considering the subface  $G$  during the running time of the algorithm (line 21), a contradiction.  $\square$

**Lemma 10.14.** *The algorithm finds all the vertices and edges of the cell.*

*Proof.* By Lemma 10.3 the algorithm terminates after a finite number of steps. Let  $(F_j)_{j=1}^s$  be the finite list of all prime subfaces. Assume by way of contradiction that some vertex  $u$  is not found. Then  $u$  corresponds to some point located on some prime subface  $F$  of the simplex, since the ray in direction  $u - p$  intersects the simplex at exactly one point, and each point on the simplex belongs to some prime subface.

Let  $p + T_1$  and  $p + T_2$  be the endpoints corresponding to the corners of  $F$ , and let  $\widetilde{L}_1, \widetilde{L}_2$  be the corresponding facets of the cell on which these endpoints are located. The facets  $\widetilde{L}_i, i = 1, 2$  are located on corresponding lines  $L_1, L_2$ . Let  $B$  the matrix from (3.1).

Assume first that  $\det(B) = 0$ . Then it must be that  $L_1 = L_2$ , since otherwise  $L_1$  and  $L_2$  are parallel and hence  $F$  is divided into two subfaces (line 14), a contradiction. However, if  $L_1 = L_2$ , then  $\widetilde{L}_1 = \widetilde{L}_2$ , and hence, by Lemma 10.11(a), the only possible vertices corresponding to  $F$  are the endpoints  $p + T_1, p + T_2$ . In particular, the missing vertex  $u$  coincides with one of these endpoints. But then, according to Lemma 10.13, the algorithm finds  $u$  as a vertex, a contradiction.

Assume now the case  $\det(B) \neq 0$ . Then  $L_1 \neq L_2$ . It must be that  $\lambda$  from (3.1) is nonnegative, since otherwise  $F$  is divided into two subfaces (line 26), a contradiction. The point of intersection between  $L_1$  and  $L_2$  is  $v = p + \lambda_1 T_1 + \lambda_2 T_2$ , and it must be in the cone corresponding to  $F$  and also in the cell of  $p$ , since otherwise  $F$  is divided into two subfaces (line 23). Hence  $v$  is a vertex corresponding to  $F$  and it is found by the algorithm at the stage when (3.1) is considered. If  $v = u$ , then the algorithm finds  $u$  when considering  $F$ , a contradiction. Hence  $v \neq u$ , and by Lemma 10.11(b) it must be that  $u$  coincides with one of the endpoints  $p + T_1$  or  $p + T_2$ . But then, according to Lemma 10.13, the algorithm finds  $u$  as a vertex, a contradiction.

Therefore all the vertices of the cell are detected. As explained in Method 5.1 and Section 6, when a vertex is detected, also the edges which intersect at it are detected. Since all the possible vertices are found by the algorithm, then so are all the possible edges.  $\square$

*Proof of Theorem 9.1.* This is a simple consequence of Lemmas 10.3,10.8,10.9,10.10, 10.12, and 10.14.  $\square$

## ACKNOWLEDGMENT

I am indebted to Omri Azencot for implementing the algorithm so expertly and for helpful discussions. I also thank Renjie Chen for helpful discussion regarding [15].

**Additional acknowledgments: to be added.**

## REFERENCES

1. A. Aggarwal, B. Chazelle, L. J. Guibas, C. O’Dúnlaing, and C. K. Yap, *Parallel computational geometry*, Algorithmica **3** (1988), 293–327, preliminary version in FOCS 1985, pp. 468–477.
2. A. Aggarwal, L. J. Guibas, J. Saxe, and P. W. Shor, *A linear-time algorithm for computing the Voronoi diagram of a convex polygon*, Discrete Comput. Geom. **4** (1989), no. 6, 591–604, A preliminary version in STOC 1987, pp. 39–45.
3. O. Aichholzer, W. Aigner, F. Aurenhammer, T. Hackl, B. Jüttler, E. Pilgerstorfer, and M. Rabl, *Divide-and-conquer for Voronoi diagrams revisited*, Proceedings of the 25th annual ACM Symposium on Computational Geometry (SoCG 2009), 2009, pp. 189–197.
4. N. M. Amato, M. T. Goodrich, and E. A. Ramos, *Parallel algorithms for higher-dimensional convex hulls*, Proceedings of the 35th IEEE Symposium on Foundations of Computer Science (FOCS 1994), 683–694.
5. N. M. Amato and F. P. Preparata, *The parallel 3D convex hull problem revisited*, Internat. J. Comput. Geom. Appl. **2** (1992), 163–173.
6. F. Aurenhammer, *Voronoi diagrams - a survey of a fundamental geometric data structure*, ACM Computing Surveys **3** (1991), 345–405.
7. F. Aurenhammer and R. Klein, *Voronoi diagrams*, Handbook of computational geometry (J. Sack and G. Urrutia, Eds.) (2000), 201–290.
8. C. B. Barber, D.P. Dobkin, and H.T. Huhdanpaa, *The Quickhull algorithm for convex hulls*, ACM Transactions on Mathematical Software **22** (1996), 469–483.
9. C. B. Barber and The-Geometry-Center, *Qhull (software)*, (2011), Copyright: 1993-2011. Web: <http://www.qhull.org>.
10. J. L. Bentley, B. W. Weide, and A. C. Yao, *Optimal expected-time algorithms for closest point problems*, ACM Trans. Math. Softw. **6** (1980), 563–580.
11. G. E. Blelloch, J. C. Hardwick, G. L. Miller, and D. Talmor, *Design and implementation of a practical parallel Delaunay algorithm*, Algorithmica **24** (1999), 243–269.
12. K. Q. Brown, *Voronoi diagrams from convex hulls*, Inf. Process. Lett. **9** (1979), 223–228.
13. ———, *Geometric transforms for fast geometric algorithms*, Ph.D. thesis, Carnegie-Mellon University, Pittsburgh, 1980.
14. T. M. Chan and E. Y. Chen, *Optimal in-place and cache-oblivious algorithms for 3-d convex hulls and 2-d segment intersection*, Computational Geometry **43** (2010), 636–646, Special issue on SoCG 2009 (a preliminary version: SoCG 2009 pp. 80–89).
15. R. Chen and C. Gotsman, *Localizing the Delaunay triangulation and its parallel implementation*, Proceedings of the 9th International Symposium on Voronoi Diagrams in Science and Engineering (ISVD 2012), 2012, Rutgers University, NJ, USA, pp. 24–31.
16. A. Chow, *Parallel algorithms for geometric problems*, Ph.D. thesis, University of Illinois, Urbana, 1980.
17. R. Cole, M. T. Goodrich, and C. O’Dúnlaing, *A nearly optimal deterministic parallel Voronoi diagram algorithm*, Algorithmica **16** (1996), 569–617.
18. T. H. Cormen, C. E. Leiserson, R. L. Rivest, and C. Stein, *Introduction to algorithms*, second ed., MIT Press and McGraw-Hill, 2001.
19. N. Dadoun and D. G. Kirkpatrick, *Parallel construction of subdivision hierarchies*, J. Comput. Syst. Sci. **39** (1989), 153–165.

20. G. B. Dantzig, *Maximization of linear function of variables subject to linear inequalities*, Activity Analysis of Production and Allocation (T. C. Koopmans, ed.), Wiley & Chapman-Hall, New York-London, 1951, pp. 339–347.
21. ———, *Linear programming and extensions*, Princeton University Press, Princeton, N.J., 1963.
22. M. de Berg, O. Cheong, M. van Kreveld, and M. Overmars, *Computational geometry: Algorithms and applications*, third ed., Springer, 2008.
23. Q. Du, M. Emelianenko, and L. Ju, *Convergence of the Lloyd algorithm for computing centroidal Voronoi tessellations*, SIAM J. Numer. Anal. **44** (2006), 102–119.
24. Q. Du, V. Faber, and M. Gunzburger, *Centroidal Voronoi tessellations: applications and algorithms*, SIAM Rev. **41** (1999), no. 4, 637–676.
25. H. Edelsbrunner, *Algorithms in combinatorial geometry*, Springer-Verlag, Berlin; New York, 1987.
26. D. J. Evans and I. Stojmenović, *On parallel computation of Voronoi diagrams*, Parallel Computing **12** (1989), 121–125.
27. S. Fortune, *A sweepline algorithm for Voronoi diagrams*, Algorithmica **2** (1987), 153–174, A preliminary version in SoCG 1986, pp. 313–322.
28. Y. Fragakis and E. Oñate, *Parallel Delaunay triangulation for particle finite element methods*, Commun. Numer. Meth. Engng. **24** (2008), 1009–1017.
29. C. Gold, *The Voronoi Web Site*, 2008, [http://www.voronoi.com/wiki/index.php?title=Main\\_Page](http://www.voronoi.com/wiki/index.php?title=Main_Page).
30. M. T. Goodrich, C. O’Dúnlaing, and C. Yap, *Computing the Voronoi diagram of a set of line segments in parallel*, Algorithmica **9** (1993), 128–141, preliminary version in LNCS WADS 1989, pp. 12–23.
31. P. J. Green and R. Sibson, *Computing Dirichlet tessellations in the plane*, Comput. J. **21** (1977), 168–173.
32. L. Guibas, D. Knuth, and M. Sharir, *Randomized incremental construction of Delaunay and Voronoi diagrams*, Algorithmica **7** (1992), 381–413, A preliminary version in ICALP 1990, pp. 414–431.
33. L. J. Guibas and J. Stolfi, *Primitives for the manipulation of general subdivisions and the computation of Voronoi diagrams*, ACM Trans. Graph. **4** (1985), 74–123.
34. C. A. R. Hoare, *Quicksort*, The Computer Journal **5** (1962), 10–16.
35. G. J. Hwang, J. M. Arul, E. Lin, and C.-Y. Hung, *Design and multithreading implementation of the wave-front algorithm for constructing Voronoi diagrams*, Distributed and Parallel Computing, vol. 3719, 2005, pp. 257–266.
36. V. Klee, *On the complexity of  $d$ -dimensional Voronoi diagrams*, Arch. Math. **34** (1980), 75–80.
37. V. Klee and G. J. Minty, *How good is the simplex algorithm?*, Inequalities III (Proceedings of the Third Symposium on Inequalities held at the University of California, Los Angeles, Calif., September 19, 1969, dedicated to the memory of Theodore S. Motzkin) (O. Shisha, ed.), Academic Press, New York-London, 1972, pp. 159–175.
38. F. Lee and R. Jou, *Efficient parallel geometric algorithms on a mesh of trees*, Proceedings of the 33rd annual ACM Southeast Regional Conference, 1995, pp. 213–218.
39. H. Meyerhenke, *Constructing higher-order Voronoi diagrams in parallel*, EWCG 2005, pp. 123–126.
40. T. Ohya, M. Iri, and K. Murota, *Improvements of the incremental methods for the Voronoi diagram with computational comparison of various algorithms*, J. Operations Res. Soc. Japan **27** (1984), 306–337.
41. A. Okabe, B. Boots, K. Sugihara, and S. N. Chiu, *Spatial Tessellations: Concepts and Applications of Voronoi Diagrams*, second ed., Wiley Series in Probability and Statistics, John Wiley & Sons Ltd., Chichester, 2000, with a foreword by D. G. Kendall.
42. J. O’Rourke, *Computational geometry in C*, Cambridge University Press, New York, 1994.

43. S. Rajasekaran and S. Ramaswami, *Optimal parallel randomized algorithms for the Voronoi diagram of line segments in the plane*, Algorithmica **33**, 436–460, a preliminary version in SoCG 1994, pp. 57–66.
44. D. Reem, *An algorithm for computing Voronoi diagrams of general generators in general normed spaces*, Proceedings of the sixth International Symposium on Voronoi Diagrams in Science and Engineering (ISVD 2009), pp. 144–152.
45. J. H. Reif and S. Sen, *Optimal parallel randomized algorithms for three dimensional convex hulls and related problems*, SIAM J. Comput. **21** (1992), 466–485, Erratum: SIAM J. Comput. **23** (1994), 447–448.
46. R. T. Rockafellar, *Convex Analysis*, Princeton Mathematical Series, Princeton University Press, Princeton, NJ, 1970.
47. O. Schwarzkopf, *Parallel computation of discrete Voronoi diagrams*, LNCS **349** (1989), 193–204, (Proc. of STACS 1989).
48. O. Setter, M. Sharir, and D. Halperin, *Constructing two-dimensional Voronoi diagrams via divide-and-conquer of envelopes in space*, Transactions on Computational Science **IX** (2010), 1–27, a preliminary version in ISVD 2009, pp. 43–52.
49. M. I. Shamos and D. Hoey, *Closet-point problems*, Proceedings of the 16th Annual IEEE Symposium on Foundations of Computer Science (FOCS 1975), pp. 151–162.
50. M. Sharir and P. Agarwal, *Davenport-Schinzel sequences and their geometric applications*, Cambridge University Press, 1995.
51. J. R. Shewchuk, *Triangle: Engineering a 2D Quality Mesh Generator and Delaunay Triangulator*, Applied Computational Geometry: Towards Geometric Engineering (Ming C. Lin and Dinesh Manocha, eds.), Lecture Notes in Computer Science, vol. 1148, Springer-Verlag, 1996, From the First ACM Workshop on Applied Computational Geometry, pp. 203–222.
52. ———, *Delaunay refinement algorithms for triangular mesh generation*, Comput. Geom. **22** (2002), 21–74.
53. D. A. Spielman and S.-H. Teng, *Smoothed analysis: Why the simplex algorithm usually takes polynomial time*, Journal of the ACM **51** (2004), 385–463, A preliminary version in STOC 2001, pp. 296–305.
54. D. A. Spielman, S.-H. Teng, and A. Üngör, *Parallel Delaunay refinement: Algorithms and analyses*, International Journal of Computational Geometry and Applications **17** (2007), 1–30.
55. C. Trefftz and J. Szakas, *Parallel algorithms to find the Voronoi diagram and the order- $k$  Voronoi diagram*, Proc. of the International Parallel and Distributed Processing Symposium (IPDPS 2003).
56. B. C. Vemuri, R. Varadarajan, and N. Mayya, *An efficient expected time parallel algorithm for Voronoi construction*, Proceedings of SPAA 1992, pp. 392–401.